Springer

KSME

Journal of Mechanical Science and Technology 29 (6) (2015) 2509~2515
www.springerlink.com/content/1738-494x(Print)/1976-3824(Online)
DOI 10.1007/s12206-015-0548-5

# Dual parallel organic Rankine cycle (ORC) system for high efficiency waste heat recovery in marine application †

Eunkoo Yun[1], Hyunjun Park[1], Sang Youl Yoon[2,*] and Kyung Chun Kim[1,*]

[1]*School of Mechanical Engineering, Pusan National University, Busan, 609-735, Korea*
[2]*Rolls-Royce and Pusan National University Technology Centre, Pusan National University, Busan, 609-735, Korea*

(Manuscript Received April 29, 2014; Revised January 24, 2015; Accepted February 14, 2015)

---

**Abstract**

A dual parallel organic Rankine cycle (ORC) system is proposed for the efficient waste heat recovery of marine applications, which present a relatively large variation of waste heat relative to sailing conditions. Simulations for single and dual ORC systems are conducted with a wide range of heat input. The performance results are compared to evaluate the benefits of the proposed dual configuration. Annual total power outputs produced by single and dual ORCs are calculated to assess the appropriateness of applying the dual ORC to a marine engine by using four models of fuel consumption distribution based on the actual sailing data of a container ship. Results demonstrate the ability of dual ORC to produce more total power output than the single ORC.

*Keywords*: Dual parallel ORC system; Marine engine; Off-design; Organic Rankine cycle; Waste heat recovery

---

## 1. Introduction

Considering the annual increase in maritime cargo, the importance of recovering waste heat has been raised in marine engineering to reduce harmful gases and save fuel [1]. As summarized in Table 1, about 40% or more of the energy consumed in a marine engine is emitted in the form of waste heat, 75% of which is discharged directly to the atmosphere in low-temperature exhaust gas and jacket coolants [2]. Recent research introduced various technologies including an organic Rankine cycle (ORC) and a thermo-electric generator (TEG) to convert engine waste heat into useful power [3].

Given the environmental issues and high energy costs leading to increased interest in the recovery of low-grade waste heat, ORC has been considered as a reliable candidate for heat recovery in various field applications such as solar thermal [4, 5], geothermal sources [6, 7] and industrial waste heat [8-10]. ORC has been widely studied for waste heat recovery in internal combustion engines including marine engines. Choi and Kim [11] suggested a dual loop configured in series for waste heat recovery in exhaust gas discharged from the main engine of a container ship. The proposed recovery system consisted of a trilateral cycle and an ORC that utilize water and R1234yf as working fluids, respectively.

Choi and Kim [11] presented the probability distributions of exhaust gas temperature and fuel consumption based on the real engine operation data of a container ship during a single one-way trip that took approximately two weeks. Fuel consumption distribution revealed that the amount of engine waste heat should indicate a large variation. Owing to the large variation of waste heat, the single ORC system can satisfy off-design conditions, where the efficiency of ORC system can be severely reduced, or the ORC system can become non-operational. Thus, the present study proposes a novel system with dual ORC loops in parallel for the efficient waste heat recovery in exhaust gas discharged from heavy-duty marine engines.

## 2. Dual ORC system in marine engine

Waste heat in the engine exhaust gas and the jacket coolant have been considered as heat sources for ORC [12]. Among these waste heat sources, the present study considers the exhaust gas as its heat source because the amount of heat in the exhaust gas is about five times larger than that in the jacket coolant as described in Table 1. Fig. 1 shows a schematic diagram of the proposed dual ORC configured in parallel to the recovery of waste heat in exhaust gas discharged from a marine engine. Exhaust gas is introduced into both ORC loops after passing through an economizer. The ORC system can be selectively operated in the dual or single modes depending on the amount of waste heat. A large amount of waste valve 2 is necessary in the dual mode to feed exhaust gas into evaporators.

*Corresponding author. Tel.: +82 51 510 2324, Fax.: +82 51 512 9835
E-mail address: kckim@pusan.ac.kr, yoonsy@pusan.ac.kr
† Recommended by Associate Editor Tong Seop Kim

Table 1. Heat balance of a 12S90ME-C9.2 standard engine (MAN diesel turbo).

| | |
|---|---|
| Fuel consumption (167 g/kWh) | 100% |
| Shaft power output | 49.3% |
| Lubricating oil | 2.9% |
| Jacket water | 5.2% |
| Exhaust gas | 25.5% |
| Air cooler | 16.5% |
| Heat radiation | 0.6% |

Table 2. Three different 200 kW ORC configurations.

| | Maximum capacity | |
|---|---|---|
| | ORC 1 | ORC 2 |
| Single ORC | 200 kW | - |
| Dual ORC 1 | 100 kW | 100 kW |
| Dual ORC 2 | 140 kW | 60 kW |

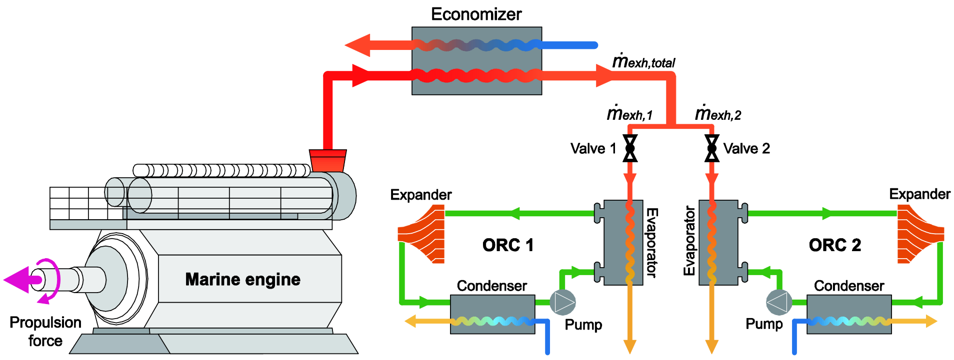


Fig. 1. Schematic diagram of a dual ORC system for recovering the waste heat of marine engine.

However, once the waste heat considerably decreases with diminished engine load, the pressure ratio between the expander inlets and outlets must be decreased in the dual mode. This action is accomplished because the mass flow rate of working fluid should be reduced to maintain vapor quality. To increase the expander inlet pressure, the exhaust gas should be concentrated into either one of the ORCs by switching to single mode. The increased pressure ratio can enhance the performance under low waste heat conditions. Hence, the dual ORC system is expected to be more effective than the single ORC, particularly in applications with large variations in waste heat.

## 3. System modeling

To evaluate the performance characteristics of the dual ORC system compared with the single ORC, three ORC systems were considered, as shown in Table 2. This study targets a 200 kW class ORC system for recovering waste heat with about 1,800 kW. R245fa was selected as the working fluid because of its suitability for the temperature range of the exhaust gas from marine diesel engine [13].

### *3.1 Expander model*

Expanders have been modeled based on the results of a CFD analysis on a radial type turbine designed for 200 kW class ORC [14]. The expander was designed with the fixed outlet pressure of 2 bar and the fixed rotational speed of 15000 rpm. Fig. 2 shows the turbine isentropic efficiency against the pressure ratio based on the CFD analysis results. Results indicate that the maximum isentropic efficiency of about 82% was achieved near the pressure ratio of approximately 6.0.

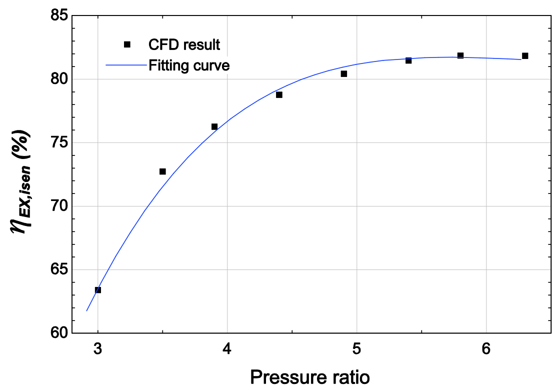


Fig. 2. Isentropic efficiency of 200 kW class turbine against pressure ratio.

The system modeling of the ORC configurations in Table 1 show the four expanders with different capacities considered, which are listed in Table 2. The isentropic efficiency against pressure ratio is assumed identical regardless of expander capacity.

The isentropic efficiency was defined as a fourth-order polynomial curve obtained by curve fitting the CFD data in Fig. 2.

$$\eta_{EX,isen} = A_1 + A_2 P_r + A_3 P_r^{\,2} + A_4 P_r^{\,3} + A_5 P_r^{\,4} \quad (1)$$

Table 3. Equation parameters for each expander.

| Capacity of expander | $V_{s,EX}$ (cm$^3$/rev) | $N_{EX}$ (rpm) | $F_{filling}$ |
|---|---|---|---|
| 200 kW | 212.54 | 15000 | 1.1 |
| 100 kW | 106.27 | | |
| 140 kW | 148.778 | | |
| 60 kW | 63.762 | | |
| Parameters for isentropic efficiency: A1 = -99.34843; A2 = 103.39882; A3 = -21.75227; A4 = 1.99596; A5 = -0.06746 | | | |

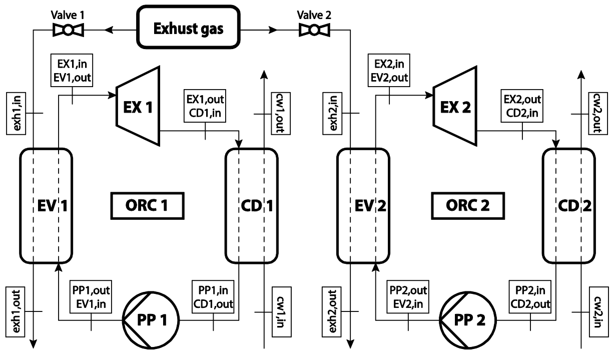


Fig. 3. Schematic of modeled dual parallel ORC system including state points.

where $P_r$ is the pressure ratio between the expander inlet and outlet. To determine the pressure at the entrance of each expander, filling factor was adopted as defined in Eq. (2).

$$F_{filling} = \frac{\dot{m}_r v_{su}}{V_{s,EX} N_{EX}} . \tag{2}$$

The filling factor was assumed as 1.1 in this study, although the filling factor was empirically determined [15]. The parameters obtained are represented in Table 3.

### 3.2 Cycle modeling

The global model of the dual ORC system was obtained by combining the expander model and the other ORC component models, including the heat source, evaporators, condensers, and pumps, as shown in Fig. 3.

The power output for each expander was calculated using Eq. (3).

$$\dot{W}_{EX} = \eta_{EX,isen} \dot{m}_r (h_{EX,in} - h_{EX,out,isen}) . \tag{3}$$

The total power output can be determined by the sum of the power outputs of ORC 1 and ORC 2. The power consumption for each working fluid pump was calculated using Eq. (4).

$$\dot{W}_{PP} = \frac{\dot{m}_r}{\eta_{PP,isen}} (h_{PP,out,isen} - h_{PP,in}) . \tag{4}$$

Table 4. Modeling parameters for ORC cycle.

| Parameter | Value |
|---|---|
| $T_{exh,in}$ [°C] | 200 |
| $\Delta T_{pinch}$ [°C] | 20 |
| $C_{p,exh}$ [kJ/kg-K] | 1.012 |
| $T_{sup}$ [°C] | 10 |
| $T_{sub}$ [°C] | 5 |
| $P_{cd}$ [bar] | 2 |
| $T_{ref}$ [°C] | 20 |
| $\eta_{PP}$ [%] | 80 |

The amount of waste heat in exhaust gas and the amount of the evaporative heat transfer can be described as Eqs. (5) and (6), respectively.

$$\dot{Q}_{exh} = \dot{m}_{exh} C_{p,exh} (T_{exh,in} - T_{exh,out}) \tag{5}$$

$$\dot{Q}_{EV} = \dot{m}_r (h_{EV,out} - h_{EV,in}) . \tag{6}$$

Cycle efficiency can be calculated with the ratio between total net power and total evaporative heat transfer as given in Eq. (7).

$$\eta_c = \frac{\dot{W}_{net,total}}{\dot{Q}_{EV,total}} = \frac{\sum (\dot{W}_{EX} - \dot{W}_{PP})}{\dot{Q}_{EV,1} + \dot{Q}_{EV,2}} . \tag{7}$$

Overall system efficiency can be calculated by considering heat effectiveness ($\varepsilon$), which represents the overall heat transfer efficiency as in Eqs. (8) and (9).

$$\varepsilon = \frac{\dot{Q}_{act}}{\dot{Q}_{\max}} = \frac{T_{exh,in} - T_{exh,out}}{T_{exh,in} - T_{ref}} \tag{8}$$

$$\eta_{overall} = \varepsilon \eta_c . \tag{9}$$

Table 4 summarizes the thermodynamic parameters of working fluid and exhaust gas. The specific heat of the exhaust gas was assumed the same with that of air at ambient condition [2]. The superheating and subcooling temperatures were kept constant, and the bottom pressure of cycle was fixed to two bars. The isentropic efficiency of the working fluid pump was assumed as the constant value of 80%. A pinch point temperature difference ($\Delta T_{pinch}$) was fixed to 20°C.

## 4. Simulation results

### 4.1 Performance characteristics

Fig. 4(a) shows power output as a function of pressure ratio for each capacity of ORC. Power output increases as pressure ratio rises. The maximum power output of each ORC can be achieved at the maximum pressure ratio. The power output against the evaporative heat transfer can be used to assess the performance of each ORC for a wide range of heat input. Fig.

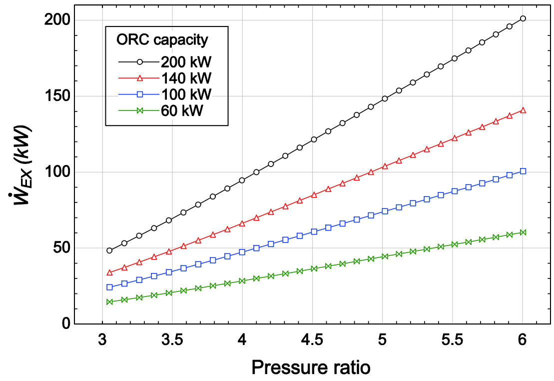


(a) Power output against pressure ratio

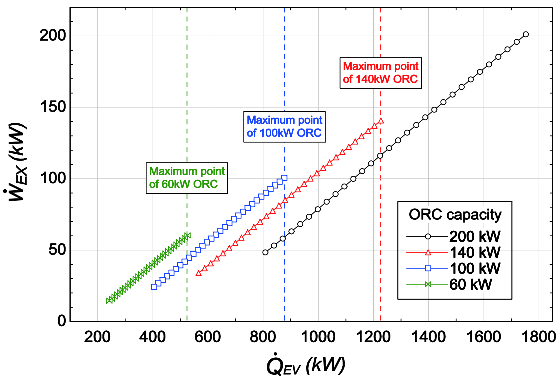


(b) Power output against the evaporative heat transfer

Fig. 4. Power outputs for ORC loops with four capacities.

4(b) clearly demonstrates that an ORC loop with less capacity can achieve increased power output with low waste heat. Thus, the dual ORC with two small ORC loops was expected to produce a higher total power output than the single ORC system by switching the operating mode. The waste heat, where the maximum power output is achieved, can be used as the operating mode change point in further dual ORC system simulations.

### 4.2 Comparison between ORC systems

To assess the appropriateness of the dual ORC system, a simulation study was conducted for large variations of waste heat. Three ORC systems were considered as listed in Table 3: a 200 kW ORC loop (Single ORC), two 100 kW ORC loops (Dual ORC 1), and 140 kW - 60 kW ORC loops (Dual ORC 2).

Given that the amount of waste heat is directly related to the exhaust gas amount, the simulated performance characteristics against the mass flow rate of the exhaust gas are graphically represented in Fig. 5. Operating mode was selected to maximize the total power output. The performance characteristics of the dual ORC system operated in dual mode should be same as those of the single ORC because of the identical expander isentropic efficiency assumption. As shown in Fig. 5(a), the dual ORC system can achieve a higher total power output than the single ORC under low waste heat conditions

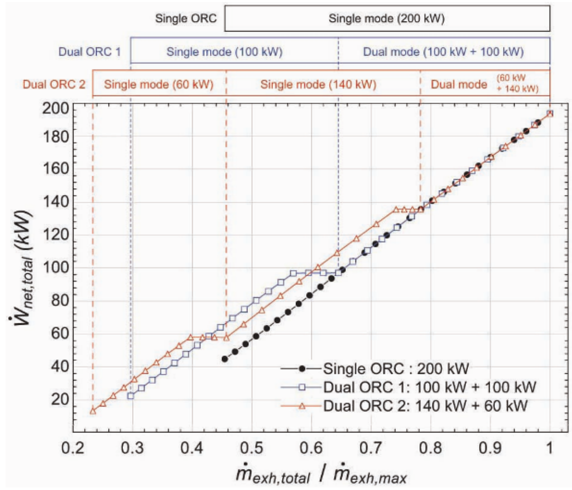


(a)

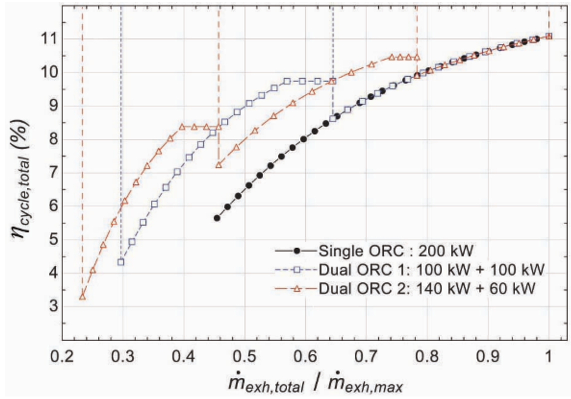


(b)

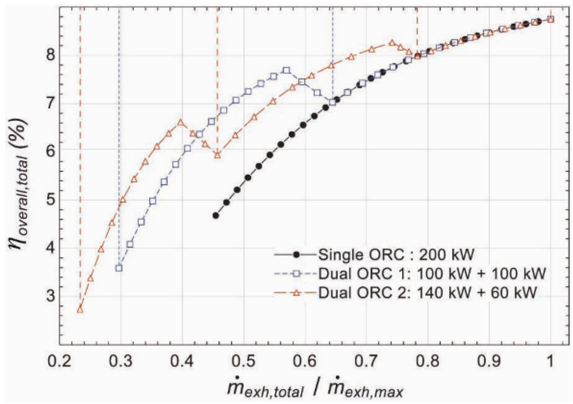


(c)

Fig. 5. Comparison of performances between single ORC and dual ORC systems.

by changing the operating mode. Results similarly show that the dual ORC system is capable of recovering a wide range of waste heat. Figs. 5(b) and (c) show that efficiencies can be improved by utilizing the dual ORC with single mode at a small amount of waste heat, and that the lower capacity ORC indicated better performance. Results further demonstrate that cycle efficiency suddenly increases with the operating mode

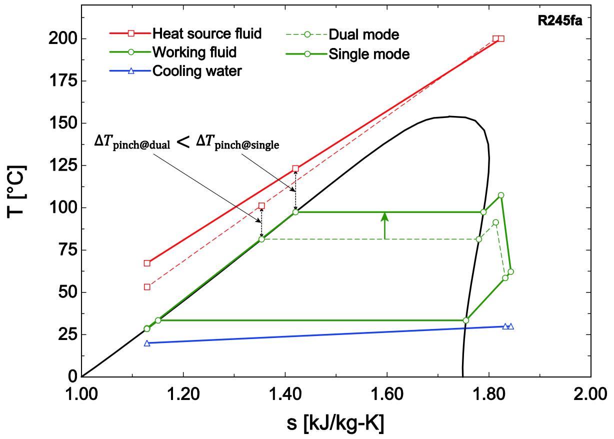


Fig. 6. T-s diagram of the cycle when operating mode changes dual mode to single mode (Dual ORC 1).

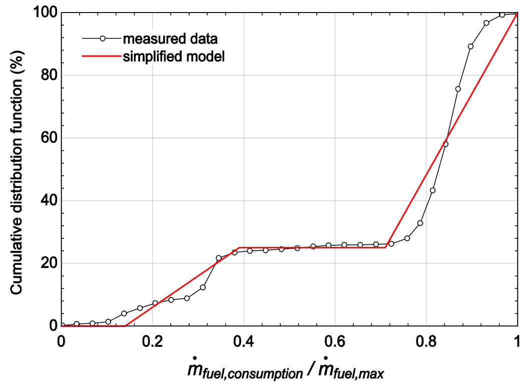


Fig. 7. Cumulative distribution of fuel consumption that is revised from Choi and Kim [11] along with a simplified model represented by a red line.

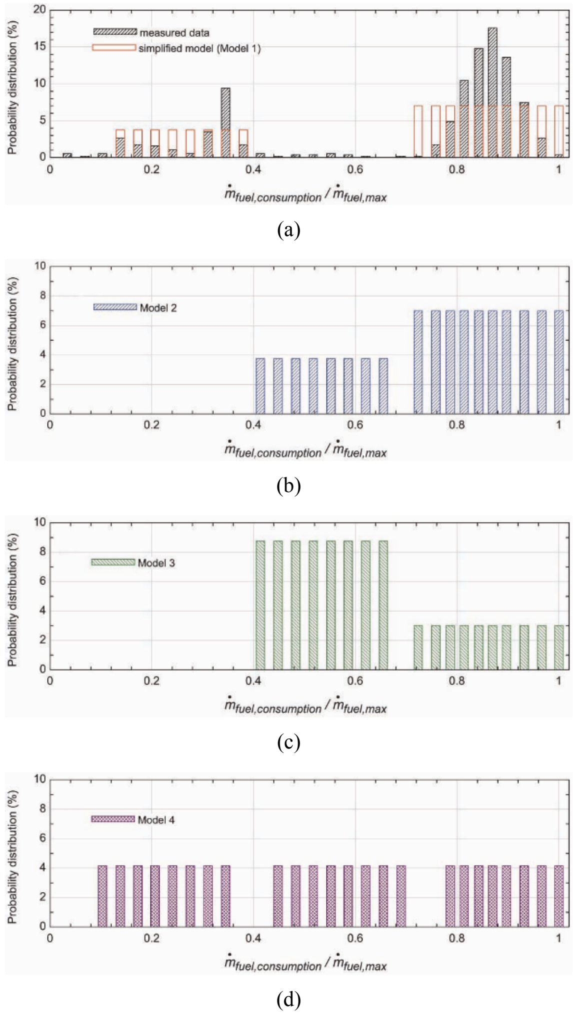


Fig. 8. Simplified probability distributions of fuel consumption.

change from dual to single mode, whereas the exhaust gas amount, the total power output, and the overall system efficiency were preserved. The sudden increase in the cycle efficiency of a single mode was caused by the decreased evaporative heat transfer for the specified power output as shown in Fig. 4(b). The reduced evaporative heat transfer imposes the outlet temperature of the exhaust gas to increase. Thus, the effectiveness of the evaporator decreases considering Eqs. (8) and (9). The simulated cycles of both modes during the mode change are presented in a T-s diagram in Fig. 6. The diagram clearly shows that the pinch point temperature difference slightly increases and that the pressure ratio rises. The increased pinch point temperature difference implies the increased outlet temperature of the exhaust gas, the reduced evaporator effectiveness, and the diminished evaporative heat transfer as described above.

## 5. Waste heat recovery of marine engine

### *5.1 Modeling of waste heat in marine engine*

A cumulative distribution of fuel consumption from the actual sailing data measured in a container ship during a one-way trip is presented in Fig. 7 [11]. The distribution shows that the waste heat of the marine engine has large variations. Thus, a general ORC system with a single design point could meet off-design conditions. The distribution addresses two main consumption regions. The distribution has been simplified for modeling the waste heat variation as presented by the red line in Fig. 7.

Fig. 8 shows the simplified probability distributions of fuel consumption. Fig. 8(a) describes the real distribution along with a simplified model (Model 1) that corresponds to a cumulative distribution in Fig. 7. For various operating conditions, three additional fuel consumption models were modified from Model 1, which have been considered in Figs. 8(b) and (c). To determine the excess heat of the exhaust gas, excess heat is assumed to be linearly proportional to fuel consumption [11].

### *5.2 Power output recovered in marine engine*

The total annual power outputs for a one-way trip achieved

Table 5. Summary of annual total power outputs for single and dual ORC systems.

| | | Unit | Actual model | Model 1 | Model 2 | Model 3 | Model 4 |
|---|---|---|---|---|---|---|---|
| Single ORC (200 kW) | Generated power | MWh | 314 | 293 | 339 | 233 | 210 |
| Dual ORC 1 (100 kW+ 100 kW) | Generated power | MWh | 330 | 304 | 360 | 281 | 234 |
| | Benefit | % | 4.93 | 3.47 | 6.63 | 15.41 | 7.60 |
| Dual ORC 2 (140 kW+ 60 kW) | Generated power | MWh | 334 | 314 | 362 | 280 | 240 |
| | Benefit | % | 6.41 | 6.79 | 7.44 | 14.97 | 9.53 |

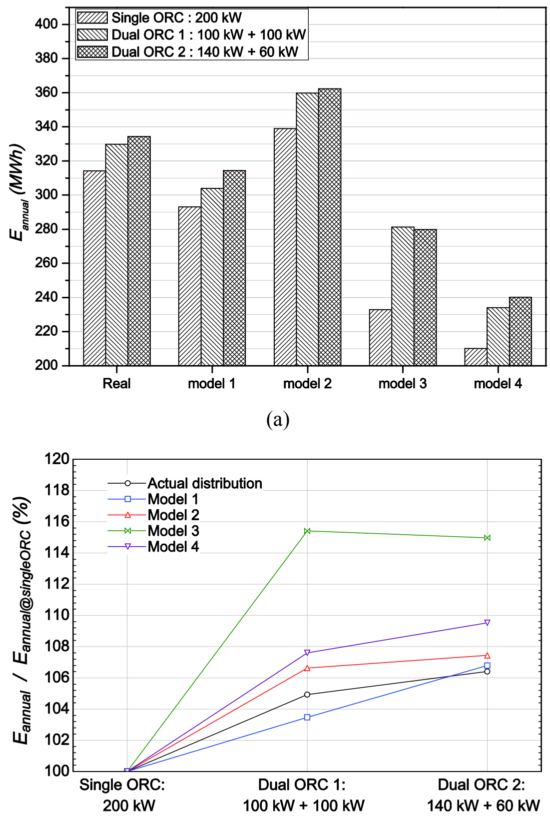


(a)

(b)

Fig. 9. Comparison of annual total power outputs for single and dual ORC systems.

in a span of two weeks were calculated using the fuel consumption models. A total of 4 round trips per year were assumed. Table 5 summarizes the total annual power outputs, $E_{annual}$ in MWh. Fig. 9 graphically shows the comparison of these amounts. The results displayed the amount of the annual total power output ranges from 223 MWh to 380 MWh, depending on the fuel consumption model and the ORC configuration. Furthermore, the results show that dual ORC systems are capable of producing more power output for all fuel consumption models compared with the single ORC. Moreover, dual ORC 2 could have taken advantage of heat recovery compared with dual ORC 1.

## 6. Conclusions

A system with dual ORC loops with a parallel configuration was proposed for efficient excess heat recovery from the exhaust gas of the marine engine, which has a large excess heat variation according to engine load. The simulation study on two different configurations of the proposed dual ORC system was conducted. The results were then compared with those of a single ORC system. The results clearly show that changing the operating mode could allow dual ORCs to achieve a higher total power output and higher efficiencies than those achieved by single ORC when the excess heat is low. The enhanced system performance was caused by an increased expander inlet pressure in the single mode of the dual ORCs.

To assess the appropriateness of applying the dual ORC to the marine engine, the annual total power outputs produced in single and dual ORCs were calculated using the actual sailing data of a container ship and four other distribution models of fuel consumption. The results showed that the dual ORC could produce more power output compared with the distribution models that can be achieved by the single ORC. The annual total power output using dual ORC configuration ranges from 103% to 115%, which is achieved by a single ORC.

Consequently, it was verified that the proposed dual ORC system has competitive advantages in recovering waste heat with large variations. Thus, the dual ORC loops parallel could be considered for marine applications, which has a large excess heat variations depending on various sailing conditions.

## Acknowledgment

This work was supported by the Basic Science Research Program (NRF-2013R1A1A2012173), GCRC-SOP (No. 2011-0030013) and Leading Foreign Research Institute Recruitment Program (NRF-2009-00495) through the National Research Foundation of Korea (NRF) by the Ministry of Science, ICT & Future Planning (MSTIP), Republic of Korea. This work was also supported by the Energy Efficiency and Resources of the Korea Institute of Energy Technology Evaluation and Planning (KETEP) granted financial resource from the Ministry of Trade, Industry & Energy, Republic of Korea (No. 20112010100030).

## Nomenclature

$C_p$ : Specific heat, kJ/kg-K
$E_{annual}$ : Annual power output, MWh
$F_{filling}$ : Filling factor
$h$ : Specific enthalpy, kJ/kg
$\dot{m}$ : Mass flow rate, kg/s
$N$ : Rotational speed, rpm
$P_r$ : Pressure ratio
$\dot{Q}$ : heat transfer, kW
$T$ : Temperature, K
$v$ : Specific volume, $m^3$/kg
$V_s$ : Swept volume/rev, $cm^3$/rev

$\dot{W}$ : Power output, kW
$\Delta T_{pinch}$ : Pinch point temperature difference, K
$\eta$ : Efficiency, %

### Subscripts

*act* : Actual amount
*c* : Cycle
*CD* : Condenser
*cw* : Cooling water
*EV* : Evaporator
*EX* : Expander
*exh* : Exhaust gas
*isen* : Isentropic
*in* : Inlet
*out* : Outlet
*PP* : Pump
*r* : Working fluid
*sup* : Superheating
*sub* : Subcooling
*overall* : System overall

## References

[1] S. Wu, Y. Cheng and Q. Ma, Discussion on ship energy-saving in low carbon economy, *Procedia Engineering*, 15 (2011) 5259-5262.
[2] B. F. Tchanche, G. Lambrinos, A. Frangoudakis and G. Papadakis, Low-grade heat conversion into power using organic Rankine cycles – A review of various applications, *Renewable and Sustainable Energy Reviews*, 15 (2011) 3963-3979.
[3] Z. Niu, H. Diao, S. Yu, K. Jiao, Q. Du and G. Shu, Investigation and design optimization of exhaust-based thermoelectric generator system for internal combustion engine, *Energy Conversion and Management*, 85 (2014) 85-101.
[4] A. M. Delgado-Torres and L. García-Rodríguez, Analysis and optimization of the low-temperature solar organic Rankine cycle (ORC), *Energy Conversion and Management*, 51 (2010) 2846-2856.
[5] J. C. Bruno, J. López-Villada, E. Letelier, S. Romera and A. Coronas, Modelling and optimisation of solar organic rankine cycle engines for reverse osmosis desalination, *Applied Thermal Engineering*, 28 (2008) 2212-2226.
[6] G. Paloso Jr. and B. Mohanty, Cascading vapour absorption cycle with organic rankine cycle for enhancing geothermal power generation, *Renewable Energy*, 3 (1993) 669-681.
[7] W. Fu, J. Zhu, T. Li, W. Zhang and J. Li, Comparison of a Kalina cycle based cascade utilization system with an existing organic Rankine cycle based geothermal power system in an oilfield, *Applied Thermal Engineering*, 58 (2013) 224-233.
[8] F. Campana, M. Bianchi, L. Branchini, A. De Pascale, A. Peretto, M. Baresi, A. Fermi, N. Rossetti and R. Vescovo, ORC waste heat recovery in European energy intensive industries: Energy and GHG savings, *Energy Conversion and Management*, 76 (2013) 244-252.
[9] I. Vaja and A. Gambarotta, Internal Combustion Engine (ICE) bottoming with Organic Rankine Cycles (ORCs), *Energy*, 35 (2010) 1084-1093.
[10] H. Tian, G. Shu, H. Wei, X. Liang and L. Liu, Fluids and parameters optimization for the organic Rankine cycles (ORCs) used in exhaust heat recovery of Internal Combustion Engine (ICE), *Energy*, 47 (2012) 125-136.
[11] B. C. Choi and Y. M. Kim, Thermodynamic analysis of a dual loop heat recovery system with trilateral cycle applied to exhaust gases of internal combustion engine for propulsion of the 6800 TEU container ship, *Energy*, 58 (2013) 404-416.
[12] M. He, X. Zhang, K. Zeng and K. Gao, A combined thermodynamic cycle used for waste heat recovery of internal combustion engine, *Energy*, 36 (2011) 6821-6829.
[13] E. H. Wang, H. G. Zhang, B. Y. Fan, M. G. Ouyang, Y. Zhao and Q.H. Mu, Study of working fluid selection of organic Rankine cycle (ORC) for engine waste heat recovery, *Energy*, 36 (2011) 3406-3418.
[14] H. S. Lim, Development of 200 kW turbine for ORC system, *Proceeding of Spring and Autumn Conference of the Korean Society of Mechanical Engineers* (2013) 279-285.
[15] S. Declaye, S. Quoilin, L. Guillaume and V. Lemort, Experimental study on an open-drive scroll expander integrated into an ORC (Organic Rankine Cycle) system with R245fa as working fluid, *Energy*, 55 (2013) 173-183.

**Eunkoo Yun** is a Ph.D. student at the School of Mechanical Engineering of Pusan National University in Korea. His research interest is energy conversion system for low-grade heat sources. He is currently in the process of developing a waste heat recovery system with increased efficiency using Organic Rankine Cycle.

**Sang Youl Yoon** is a Research Professor in Rolls Royce-Pusan National University Technology Centre in Korea. His research interests include aero-thermal measurement and heat management system.

**Kyung Chun Kim** is a Professor at the School of Mechanical Engineering of Pusan National University in Korea. He obtained his Ph.D. from the Korea Advanced Institute of Science and Technology (KAIST), Korea, in 1987. He was selected as a Member of the National Academy of Engineering of Korea in 2004. His research interests include flow measurements based on PIV/LIF, POCT development, wind turbines, and organic Rankine cycle system.